Spring Technical Meeting
Eastern States Section of the Combustion Institute
March 10-13, 2024
Athens, Georgia

Extinction of Premixed Counterflow Ammonia-Air Flames

Paul Papas[1,], James F. Stevens[2], Ruozhou Fang[2], Chih-Jen Sung[2], Lance L. Smith[1]*

[1]RTX Technology Research Center, E. Hartford, CT 06117, USA
[2]University of Connecticut, Storrs, CT 06269, USA
[*]Corresponding Author Email: paul.papas@rtx.com

Abstract: The effects of radiative heat loss and pressure on premixed counterflow ammonia-air flames have been investigated as a function of equivalence ratio. Non-adiabatic counterflow premixed flame simulations incorporating detailed chemistry, transport and radiative heat transfer in the optically thin limit have been employed to elucidate important underlying physics and extinction characteristics. Non-adiabatic counterflow premixed computations show that the combined effects of positive flame stretch and radiative heat loss for sub-unity Lewis number mixtures lead to the extension of the lean flammability limit for ammonia-air flames, revealing a C-shaped curve near the lean flammability limit that exhibits both radiative-induced and stretch-induced extinction states. The computations compare favorably with the experimentally determined extinction stretch rate values for the stretch-induced extinction states over a wide range of equivalence ratios at different pressures up to 6 atm.
Keywords: Ammonia, Extinction, Counterflow flames, Radiative loss

1. Introduction

Ammonia, a promising carbon-free fuel, requires significantly more energy to ignite and exhibits weaker flame stability as compared to typical hydrocarbon fuels. Although previous work has investigated some key features of ammonia combustion at elevated pressures [e.g., 1-4], fundamental combustion properties of pure ammonia flames at elevated pressures and temperatures in general, including burning velocities and extinction limits, are still sparse. The determination of the fundamental flammability limits for weakly burning premixed flames such as ultra lean hydrocarbon flames or ammonia flames is of practical importance. The counterflow technique has been widely used for experimentally determining fundamental premixed flame characteristics. In principle, the fundamental flammability limits could also be determined for counterflow premixed flames by measuring the extinction stretch rates with progressively weaker fuel concentrations. The major assumption in such an approach is that the extinction stretch rate varies linearly with concentration very near the fundamental flammability limit. As demonstrated in [5] using counterflow premixed flame simulations with detailed chemistry/transport and radiative heat loss, the authors were able to quantify the different extinction mechanisms for lean or rich hydrocarbon flames, assess the influence of stretch-radiation on the extinction of such near-limit flames, and identify the modification of the fundamental limits.

The current study aims to investigate the combined effects of stretch and radiative heat loss on the response and extinction of counterflow ammonia-air flames over a wide range of equivalence ratios and pressures, including the existence of dual-extinction states (stretch- and radiation-induced) for near-limit lean flames and the extension of the fundamental lean flammability limit. Furthermore, while there are several chemical kinetic models in the literature for modelling ammonia flame behavior and structure, it is known that they vary substantially in their predictions.

These discrepancies, which can be especially large, prevent use of models to reliably predict ammonia flame structure and extinction limits without validation. As a result, another objective of this work is to provide extinction limit data on premixed ammonia-air flames at varying pressures and equivalence ratios to provide anchor points for model validation and refinement.

2. Experimental Specifications

Extinction conditions were determined experimentally in a co-axial nozzle counterflow configuration. The present opposed jet burner setup is described briefly here, and details can be found in [6]. The separation distance L between the nozzle exits was maintained at 10.4 mm. Experiments were performed with ammonia (>99.9% purity) and air from an in-house air supply equipped with dryer along with an in-line cleaner/dryer installed in the flow system. To prevent edge effects, nitrogen (99.99% purity) was introduced in both outer co-axial nozzle flows. The flow rates of the ammonia and air gases were set with mass flow controllers that had a full-scale accuracy of 0.2% and 0.8% reading. The initial temperature for the reactant temperature at the nozzle exits ranged from 294–298 K. The vessel pressure was measured with a pressure transducer with a reported ±0.05% accuracy of the reading. For a given equivalence ratio (ϕ), extinction was accomplished by gradually increasing the velocity of both the upper and lower nozzle streams, while maintaining the twin luminous flame locations midway between the nozzle exits. A global stretch rate experienced by the flame in a symmetric twin-flame configuration is defined as $\kappa = 4V/L$, where V is the the mean normal velocity at the nozzle exit taken as the area-averaged nozzle exit velocity based on the measured mass flowrate of the reactant mixture. For the conditions of this work, it is found that the local and global stretch rates differ by less than 4%. Propagation of error analyses and experimental repeatability were used to determine reported uncertainties.

3. Computational Specifications

The twin counterflow premixed flames were modelled using the *CounterflowDiffusionFlame* module of Cantera [7] adapted for the twin premixed flame configuration. In the optically-thin limit, the radiative heat loss per unit volume is modeled as $q_r = -4\sigma\kappa_p(T^4 - T_o^4)$, where σ is the Stefan-Boltzmann constant, κ_p is the total Planck mean absorption coefficient of the gas, T is the local temperature, and T_o is the ambient temperature taken as the unburnt reactant temperature. In general, the total Planck mean absorption coefficient is given by $\kappa_p = \sum \kappa_i p_i$, where p_i is partial pressure of the radiating gaseous species. Here, the only radiating species considered is gaseous water, the major combustion product species from ammonia-air combustion, and its Planck mean absorption coefficient was taken from Tien [8]. Recently, Nakamura and Shindo [9] used updated Planck mean absorption coefficients for H_2O, NO, N_2O, and NH_3 to compute the unstretched laminar flame speeds for freely propagating ammonia-air flames with radiative heat loss in the optically thin limit. Using the same chemical kinetic model employed by [9] and *only* water as the radiating species, we were able to reproduce the laminar flame speeds for ammonia-air mixtures reported in [9] to well within 2%; thus, the radiative contributions from NO, N_2O, and NH_3 are negligible since their concentration levels are relatively low in the high-temperature flame regions.

For the counterflow flame configuration, we employed an automated script to generate the unstable branches near the extinction turning points in an efficient manner. The nozzle separation distance was fixed at 10 cm to ensure there was no upstream conductive heat loss to the nozzle boundary for the near-limit flames studied. The reaction mechanism used for this counterflow ammonia combustion study was taken from Stagni et al. [10]. The other published chemical kinetic models for H/N/O systems that were implemented and considered were those developed by Glarborg and co-workers [11,12] and Powell et al. [13,14].

4. Results and Discussion

Figure 1(a) shows the maximum flame temperature calculated as a function of the stretch rate κ for lean ammonia-air (ϕ=0.7) flames at 1 atm, with and without radiative heat loss. The reported lean flammability limit for ammonia-air mixtures ranges from ϕ=0.59 [15] to ϕ=0.71 [16] at ambient conditions. As observed for lean methane-air flames with Lewis number < 1 [5], positively stretched flames can persist with burning beyond the lean flammability limit for the unstretched freely propagating flame. For the adiabatic condition without radiative heat loss, the maximum flame temperature initially increases with positive stretch due to the non-equidiffusion effects, and then decreases due to incomplete reaction as the extinction state $\kappa_{ext,ad}$ (87.6 s^{-1}) is approached, as shown in Fig. 1(a). When unstretched, the maximum flame temperature degenerates to the adiabatic flame temperature T_{ad} (1730.5 K). Whereas the non-adiabatic flames exhibit an isola response, with dual extinction turning points that are designated as $\kappa_{ext,S}$ and $\kappa_{ext,R}$ in Fig. 1(a) for the higher and lower values of κ, respectively. The higher or stretch-induced extinction state $\kappa_{ext,S}$ (81.2 s^{-1}) arises from the additional radiative loss that facilitates extinction such that $\kappa_{ext,S}<\kappa_{ext,ad}$. The lower extinction turning point corresponds to the radiation-induced extinction state $\kappa_{ext,R}$ (1.3 s^{-1}) and arises due to progressively increasing radiative heat loss with decreasing stretch rate [5]. Consequently, steady burning solutions are not possible below $\kappa_{ext,R}$ at equivalence ratios less than the lean flammability limit for unstretched (freely propagating) flames. Figure 1(b) further shows the variation of the computed separation distance between the twin premixed flames, determined from the local maximum heat release rate location, with κ for a fixed ϕ=0.7. It is seen from Fig. 1(b) that the adiabatic counterflow twin flames are far apart at low stretch rates and approach the stagnation surface with increasing stretch rate. On the other hand, the variation of the non-adiabatic flame separation distance shows a non-monotonic behavior with both stretch- and radiation-induced extinction states, $\kappa_{ext,S}$ and $\kappa_{ext,R}$, occurring when the twin flames merge.

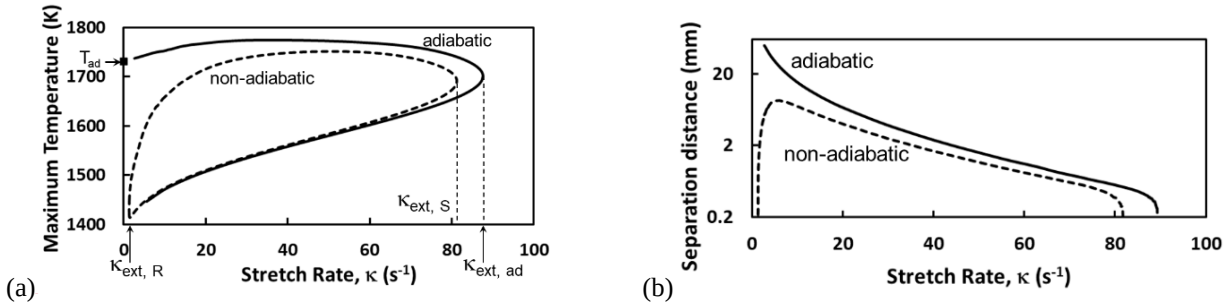

Figure 1. Computed (a) maximum flame temperature and (b) flame separation distance as a function of the stretch rate κ for near-limit, lean ammonia-air (ϕ=0.7) flames at 1 atm with and without radiative heat loss.

Figure 2(a) plots the computed maximum flame temperature as a function of the stretch rate κ for lean and stoichiometric ammonia-air flames. For each equivalence ratio, the solid and dashed lines correspond to adiabatic and non-adiabatic (with radiative heat loss) flames, respectively. As discussed previously, the stretch-induced extinction state $\kappa_{ext,S}<\kappa_{ext,ad}$ for a given ϕ because the additional radiative heat loss facilitates extinction. For the stoichiometric case, the non-adiabatic stretch rate at extinction is 5% lower than that of the corresponding adiabatic flame and increases to about 24% lower for the ϕ=0.6 condition. Also, both the fuel-lean flames of ϕ=0.6 and 0.7 exhibit radiative-induced extinction states, $\kappa_{ext,R}$, whereas the ϕ=0.8 and 1.0 flames do not.

Figure 2(b) plots the computed $\kappa_{ext,S}$ and $\kappa_{ext,R}$ as a function of ϕ for counterflow ammonia-air flames at both 1 atm (black color) and 5 atm (blue color), as well as the extinction stretch rate data

reported by Colson et al. [4] (solid symbols) and the experimental data obtained in this study (open symbols). Figure 3(a) replots the stretch-induced extinction data in Fig. 2(b) using a linear y-axis scale. At 1 atm, the computed non-adiabatic results at the stretch-induced extinction state overpredict these data by up to 30%. At 5 atm, on the other hand, the computed stretch-induced extinction stretch rates fall between the Colson et al. [4] and current data sets. From ϕ=0.58 to about ϕ=0.73 at 1 atm, Fig. 2(b) shows that both computed stretch-induced and radiation-induced extinction states exist, whereas only stretch-induced extinction states exist for ϕ>0.73. The variation of these dual extinction stretch rates forms a C-curve, whereby steady burning counterflow ammonia-air flames cannot be established below ϕ=0.58. This predicted lean-limit of ϕ=0.58 at 1 atm for the stretched counterflow premixed ammonia-air flames is lower ("extended") than that for planar, freely propagating premixed flames without stretch, computed to be around ϕ=0.73. Furthermore, Fig. 2(b) shows that although experimental and computed stretch-induced extinction stretch rates at 5 atm are much higher than those at 1 atm, the extended lean limits of flammability for counterflow ammonia-air flames are close in the pressure range investigated.

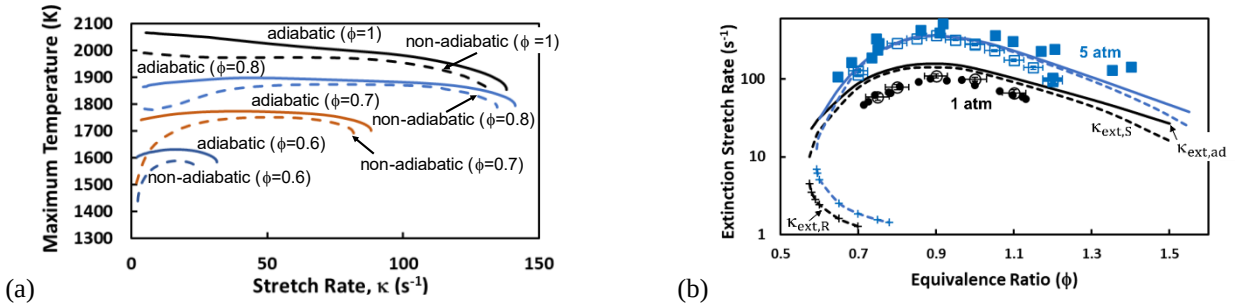

Figure 2. (a) Computed maximum flame temperature as a function of the stretch rate κ for lean and stoichiometric ammonia-air flames with and without radiative heat loss. (b) C-shaped curves for counterflow premixed fuel-lean, ammonia-air flames at 1 and 5 atm showing computed $\kappa_{ext,ad}$ (solid lines), $\kappa_{ext,S}$ (dashed lines), and $\kappa_{ext,R}$ (dashed lines with +). Experimental data from [4] (solid symbols) and this study (open symbols) are shown for comparison.

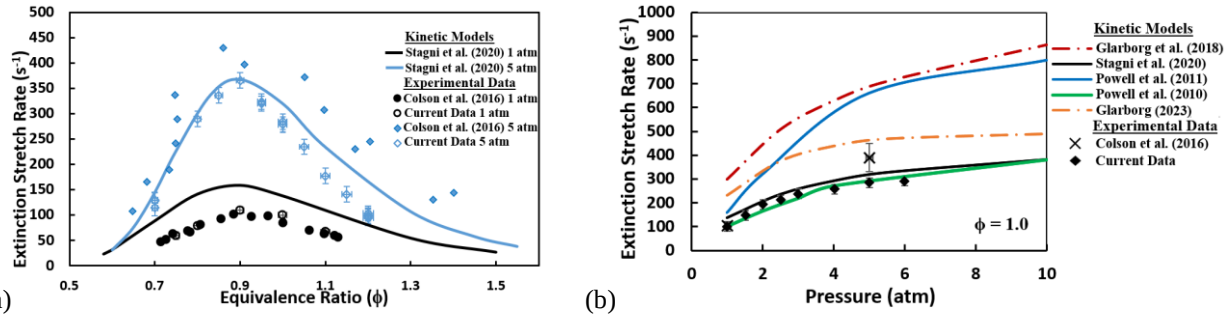

Figure 3. (a) Extinction stretch rate versus equivalence ratio at 1 and 5 atm comparing computed results (line) as well as experimental data of Colson et al. [4] (filled symbols) and the current work (open symbols). (b) Computed (lines) and experimental data (symbols) extinction stretch rate versus pressure for stoichiometric ammonia-air flames.

Figure 3(b) compiles a series of numerical simulations from this study utilizing various kinetic models and compares them against our experimental data as well as the data from Colson et al. [4]. The comparison shows that the predictions from chemical kinetic models of Stagni et al. [10] and Powell et al. [13] agree with experimental data, whereas the other chemical kinetic models overpredict the extinction stretch rate data for the conditions studied. Notably, it is shown that the models of Stagni et al. [10] and Powell et al. [13] also capture the "bending" in the extinction stretch rate curve with respect to pressure shown in Fig. 3(b). More experimental datasets covering a wider range of flame conditions are required to guide future model refinement efforts.

5. Conclusions

Both numerical and experimental studies of counterflow premixed ammonia-air flame extinction were conducted at elevated system pressures. Numerical simulations using detailed chemical and transport descriptions with an optically thin radiation model incorporated were used to elucidate the effects of radiative heat loss on the extinction state. Non-adiabatic counterflow premixed flame computations reveal the existence of both radiation-induced as well as stretch-induced extinction states near the fuel lean limit for ammonia-air flames, giving rise to a C-shaped curve when plotting extinction stretch rate as a function of equivalence ratio. The extension of the lean flammability limit for stretched ammonia-air flames, even at high pressures, may have practical implications for the operability and stability of ammonia combustors. In consideration of experimental uncertainties, our experimentally determined extinction stretch rate values for the stretched-induced extinction state at system pressures up to 6 atm compare favorably with computations using the baseline chemical kinetic model selected. Additional work is required, however, to validate comprehensive N/H mechanisms at elevated temperature and pressure conditions.

6. Acknowledgements

This research was funded by the Department of Energy under Award Number DE-FE0032169.

7. References

[1] H. Dai, J. Wang, X. Cai, S. Su, H. Zhao, Z. Huang, Lewis number effects on laminar and turbulent expanding flames of NH_3/H_2/air mixtures at elevated pressures, *Proc Combust. Inst.* 39(2) (2023) 1689-1697.

[2] K.P. Shrestha, C. Lhuillier, A.A. Barbosa, P. Brequigny, F. Contino, C. Mounaïm-Rousselle, F. Mauss, An experimental and modeling study of ammonia with enriched oxygen content and ammonia/hydrogen laminar flame speed at elevated pressure and temperature, *Proc Combust. Inst.* 38(2) (2021) 2163-2174.

[3] G. Wang, H. Tang, C. Yang, G. Magnotti, W.L. Roberts, T.F. Guiberti, Quantitative laser-induced fluorescence of NO in ammonia-hydrogen-nitrogen turbulent jet flames at elevated pressure, *Proc Combust. Inst.* 39(1) (2023) 1465-1474.

[4] S. Colson, A. Hayakawa, T. Kudo, H. Kobayashi, Extinction characteristics of ammonia/air counterflow premixed flames at various pressures, *J. Thermal Sci. Tech.* 11(3) (2016) JTST0048-JTST0048.

[5] C.J. Sung, C.K. Law, Extinction mechanisms of near-limit premixed flames and extended limits of flammability, *Proc. Combust. Inst.* 26 (1996) 865-873.

[6] X. Hui, C.J. Sung, Laminar flame speeds of transportation-relevant hydrocarbons and jet fuels at elevated temperatures and pressures, *Fuel* 109 (2013) 191-200.

[7] D.G. Goodwin, R.L. Speth, H.K. Moffat, B.W. Weber, Cantera: An object-oriented software toolkit for chemical kinetics, thermodynamics, and transport processes, Cantera, Version 2.6.0, (2022), https://www.cantera.org.

[8] C.L. Tien., In: *Adv. Heat Trans*., Vol. 5, New York: Academic Press, (1968) 253–324. See also, C.L. Hubbard and C.L Tien, *ASME J. Heat Trans.* 100 (1978) 235-239.

[9] H. Nakamura, M. Shindo, Effects of radiation heat loss on laminar premixed ammonia/air flames, *Proc. Combust. Inst.* 37 (2019) 1741–1748.

[10] A. Stagni, C. Cavallotti, S. Arunthanayothin, Y. Song, O. Herbinet, F. Battin-Leclerc, T. Faravelli, An experimental, theoretical and kinetic-modeling study of the gas-phase oxidation of ammonia, *React. Chem. Eng.* 5 (2020) 696-711.

[11] P. Glarborg, J.A. Miller, B. Ruscic, S.J. Klippenstein, Modeling nitrogen chemistry in combustion, *Prog. Energy Combust. Sci*. 67 (2018) 31–68.

[12] P. Glarborg, The $NH_3/NO_2/O_2$ system: Constraining key steps in ammonia ignition and N_2O formation, *Combust. Flame* 257(1) (2023) 112311.

[13] O.A. Powell, P. Papas, C. Dreyer, Hydrogen- and C_1–C_3 hydrocarbon-nitrous oxide kinetics in freely, propagating and burner stabilized flames, shock tubes, and flow reactors, *Combust. Sci. Tech.* 182 (2010) 252–283.

[14] O.A. Powell, P. Papas, C. Dreyer, Flame structure measurements of NO in premixed hydrogen-nitrous oxide flames, *Proc. Combust. Inst.* 33 (2011) 1053–1062.

[15] K. Zhang, S. Shang, X. Li, W. Gao, Lower flammability limits of NH_3/H_2 mixtures under different initial temperatures and initial pressures, *Fuel* 331 (2023) 125982.

[16] G. Ciccarelli, D. Jackson, J. Verreault, Flammability limits of NH_3–H_2–N_2–air mixtures at elevated initial temperatures, *Combust. Flame* 144, (2006) 53–63.